Johnbosco C. Egbueri
Joshua O. Ighalo
Chaitanya B. Pande *Editors*

Climate Change Impacts on Nigeria

Environment and Sustainable Development

Springer

Springer Climate

Series Editor

John Dodson, Institute of Earth Environment, Chinese Academy of Sciences, Xian, Shaanxi, China

Contents

Hammadi M, Fehem A, Harrabi H, Ayeb N, Khorchani T, Salama AAK, Casals R, Such X, Caja G (2012) Shading effects on respiratory rate and rectal temperature in Tunisian local goat kids during summer season. In: Proceedings of XI international conference on goats, Gran Canaria, Spain, 23–27 Sept 2012, p 127

Hansen PJ (2014) Current and future assisted reproductive technologies for mammalian farm animals. In: Current and future reproductive technologies and world food production. Springer, New York, NY, pp 1–22

Hendrix CS (2017) The streetlight effect in climate change research on Africa. Glob Environ Chang 43:137–147

Herrero M, Havlík P, McIntire J, Palazzo A, Valin H (2014) African Livestock Futures: Realizing the potential of livestock for food security, poverty reduction and the environment in Sub-Saharan Africa. Office of the Special Representative of the UN Secretary General for Food Security and Nutrition and the United Nations System Influenza Coordination. (UNSIC) Geneva, Switzerland

Hetherington JB, Wiethoelter AK, Negin J, Mor SM (2017) Livestock ownership, animal source foods and child nutritional outcomes in seven rural village clusters in Sub-Saharan Africa. Agric Food Secur 6(1):9

Hoffman T, Vogel C (2008) Climate change impacts on African rangelands. Rangelands 30(3):12–17

Hoffmann I (2010) Climate change and the characterization, breeding and conservation of animal genetic resources. Anim Genet 41:32–46

Hopkins A, Del Prado A (2007) Implications of climate change for grassland in Europe: impacts, adaptations and mitigation options: a review. Grass Forage Sci 62(2):118–126

IPCC (2014b) Summary for policymakers. In: Climate change 2014: impacts, adaptation, and vulnerability. Part A: global and sectoral aspects. Contribution of working group II to the fifth assessment report of the intergovernmental panel on climate change. In: Field CB, Barros VR, Dokken DJ, Mach KJ, Mastrandrea MD, Bilir TE, Chatterjee M, Ebi KL, Estrada YO, Genova RC, Girma B, Kissel ES, Levy AN, MacCracken S, Mastrandrea PR, White LL (eds). Cambridge University Press, Cambridge, United Kingdom and New York, NY, USA, pp 1–32

IPCC (2014a) Mitigation of climate change. In: Edenhofer O, Pichs-Madruga R, Sokona Y, Farahani E, Kadner S, Seyboth K, Adler A, Baum I, Brunner S, Eickemeier P, Kriemann B, Savolainen J, Schlömer S, von Stechow C, Zwickel T, Minx JC (eds.) Climate change 2014a: mitigation of climate change. Contribution of working group III to the fifth assessment report of the intergovernmental panel on climate change. Cambridge University Press, Cambridge, United Kingdom and New York, NY, USA

Katiyatiya CLF, Muchenje V, Mushunje A (2014) Farmers' perceptions and knowledge of cattle adaptation to heat stress and tick resistance in the Eastern Cape, South Africa. Asian Australas J Anim Sci 27(11):1663–1670

Kaugama HH, Ahmed BA (2014) Prospect and challenges of farming along the Hadejia-Nguru Wetland in Jigawa State Nigeria. Int J Acad Res Econ Manag Sci 3(6):43

Kebede D (2016) Impact of climate change on livestock productive and reproductive performance. Livestock Res Rural Dev 28:227

Kekana TW, Nherera-Chokuda FV, Muya MC, Manyama KM, Lehloenya KC (2018) Milk production and blood metabolites of dairy cattle as influenced by thermal-humidity index. Trop Anim Health Prod 50:921–924

Kumar S, Kumar B, Hindustani S, Sankhala G (2011) Knowledge level of dairy farmers in operational area of Krishi Vigyan Kendra about improved dairy farming practices. Res J Agric Sci 2(1):122–124

Kurukulasuriya P, Mendelsohn R, Hassan R, Benhin J, Deressa T, Diop M, Dinar A et al (2006) Will African agriculture survive climate change?. World Bank Econ Rev 20(3):367–388

Lumbroso D (2018) How can policy makers in sub-Saharan Africa make early warning systems more effective? The case of Uganda. Int J Disaster Risk Reduct 27:530–540

Mader TL, Davis MS (2004) Effect of management strategies on reducing heat stress of feedlot cattle: feed and water intake. J Anim Sci 82:3077–3087

Makkar HP (2016) Smart livestock feeding strategies for harvesting triple gain–the desired outcomes in planet, people and profit dimensions: a developing country perspective. Anim Prod Sci 56(3):519–534

Malau-Aduli BS, Eduvie LO, Lakpini CAM, Malau-Aduli AEO (2003) Variations in liveweight gains, milk yield and composition of Red Sokoto goats fed crop-residue-based supplements in the subhumid zone of Nigeria. Livest Prod Sci 83(1):63–71

Mapiye C, Chimonyo M, Dzama K, Raats JG, Mapekula M (2009) Opportunities for improving Nguni cattle production in the smallholder farming systems of South Africa. Livest Sci 124(1–3):196–204

Mapiye O, Chikwanha OC, Makombe G, Dzama K, Mapiye C (2020) Livelihood, food and nutrition security in Southern Africa: What role do indigenous cattle genetic resources play? Diversity 12(2):74

McDermott JJ, Kristjanson PM, Kruska RL, Reid RS, Robinson TP, Coleman PG, Jones PG, Thornton PK (2002) Effects of climate, human population and socio-economic changes on tsetse-transmitted trypanosomiasis to 2050. In: The African trypanosomes. Springer, Boston, MA, pp 25–38

McIntire J, Bourzat D, Prabhu P (1992) Crop-livestock interaction in sub-Saharan Africa. World Bank, Washington, DC

Meltzer MI (1995) Livestock in Africa: the economics of ownership and production, and the potential for improvement. Agric Hum Values 12(2):4–18

Mengesha M (2016) Effect of graded levels of Tagasaste (Chamaecytisus palmensis) leaves supplementation on performance of yearling Menz sheep in Ethiopian Highlands. MSc thesis in Animal and Range Sciences (Specialization: Animal Nutrition). Hawassa University, Hawassa, Ethiopia

Muller CJC, Botha JA, Coetzer WA, Smith WW (1994a) Effect of shade on various parameters of Friesian cows in a Mediterranean climate in South Africa. 2. Physiological responses. South Afric J Anim Sci 24:56–60

Muller CJC, Botha JA, Smith WW (1994b) Effect of shade on various parameters of Friesian cows in a Mediterranean climate in South Africa. 2. Physiological responses. South Afric J Anim Sci 24:61–66

Musemwa L, Mushunje A, Chimonyo M, Mapiye C (2010) Low cattle market off-take rates in communal production systems of South Africa: causes and mitigation strategies. J Sustain Dev Afr 12:209–226

Naqvi SMK, Sejian V (2011) Global climate change: role of livestock. Asian J Agric Sci 3(1):19–25

Nhamo L, Mabhaudhi T, Modi AT (2019) Preparedness or repeated short-term relief aid? Build Drought Resil through Early Warn South Afr 45(1):75–85

Ogenga JO, Mugalavai EM, Nyandiko NO (2018) Impact of rainfall variability on food production under rainfed agriculture in Homa Bay County, Kenya. Int J Res Sci Publ 861

Okouruwa MI (2015) Effect of coat characteristics on physiological traits and heat tolerance of West African Dwarf sheep in Southern Nigeria. Open J Anim Sci 5:351–357

Onzima RB, Upadhyay MR, Doekes HP, Brito LF, Bosse M, Kanis E, Groenen MAM, Crooijmans RPMA (2018) Genome-wide characterization of selection signatures and runs of homozygosity in Ugandan goat breeds. Front Genet 9:1–13. https://doi.org/10.3389/fgene.2018.00318

Otte J, Costales A, Dijkman J, Pica-Ciamarra U, Robinson T, Ahuja V, Ly C, Roland-Holst D (2012) Livestock sector development for poverty reduction: an economic and policy perspective–livestock's many virtues. FAO (Food and Agriculture Organization of the United Nations), Rome, Italy, pp 161

Palmer AR, Bennett JE (2013) Degradation of communal rangelands in South Africa: towards an improved understanding to inform policy. Afr J Range Forage Sci 30(1–2):57–63

Patel SJ, Patel MD, Patel JH, Patel AS, Gelani RN (2016) Role of women gender in livestock sector: a review. J Livest Sci 7:92–96

Patz JA, Confalonieri UE, Amerasinghe FP, Chua KB, Daszak P, Hyatt AD, Molyneux D, Thomson M, Yameogo L, Lazaro MM, Vasconcelos P (2005) Human health: ecosystem regulation of infectious diseases. In: Ecosystems and human well-being: current state and trends: findings of

the condition and trends working group of the millennium ecosystem assessment, vol 14, pp 391-415. (Dec 2005)

Pica-Ciamarra U, Baker D, Morgan N, Ly C, Nouala S (2013) Investing in African livestock: business opportunities in 2030–2050. Livestock data innovation in Africa Project. A joint initiative of the World Bank, FAO, ILRI, AU-IBAR with support from the Bill and Melinda Gates Foundation, Seattle, WA, p 1–14

Pollock DSG, Green RC, Nguyen T (1999) Handbook of time series analysis, signal processing and dynamics. Elsevier, New York, USA, p 848. ISBN-13: 9780080507873

Raheem D, Carrascosa C, Oluwole OB, Nieuwland M, Saraiva A, Millán R, Raposo A (2019) Traditional consumption of and rearing edible insects in Africa, Asia and Europe. Crit Rev Food Sci Nutr 59(14):2169–2188

Renaudeau D, Collin A, Yahav S, De Basilio V, Gourdine JL, Collier RJ (2012) Adaptation to hot climate and strategies to alleviate heat stress in livestock production. Animal 6(5):707–728

Roessler R, Mpouam S, Muchemwa T, Schlecht E (2016) Emerging development pathways of urban livestock production in rapidly growing West Africa cities. Sustainability 8(11):1199

Rojas-Downing MM, Nejadhashemi AP, Harrigan T, Woznicki SA (2017a) Climate change and livestock: Impacts, adaptation, and mitigation. Clim Risk Manag 16:145–63. (1 Jan 2017a)

Rojas-Downing MM, Nejadhashemi AP, Harrigan T, Woznicki SA (2017b) Climate change and livestock: impacts, adaptation, and mitigation. Clim Risk Manag 16:145–163

Rosegrant MW, Cai X, Cline SA (2002) World water and food to 2025: dealing with scarcity. Int Food Policy Res Inst

Ruel MT, Quisumbing AR, Balagamwala M (2017) Nutrition-sensitive agriculture: What have we learned and where do we go from here? Int Food Policy Res Inst 1681

Rust JM, Rust T (2013) Climate change and livestock production: a review with emphasis on Africa. S Afr J Anim Sci 43(3):256–267

Ryan SJ, McNally A, Johnson LR, Mordecai EA, Ben-Horin T, Paaijmans K, Lafferty KD (2015) Mapping physiological suitability limits for malaria in Africa under climate change. Vector-Borne Zoonotic Dis 15(12):718–725

Salem BM, Bouraoui R (2009) Heat stress in Tunisia, effects on dairy cows and potential means of alleviating it. S Afr J Anim Sci. 39:256–259

Sarangi S (2018) Adaptability of goats to heat stress: a review. Pharma Innov J 7(4):1114–1126

Scholtz M, Pyoos G, Seshoka M, Theunissen A (2018) The effect of climate on the pre- and post-weaning performance of different beef cattle genotypes. J Anim Sci 96:521. (suppl Supplement 3; Champaign)

Scholtz MM, Theunissen A (2010) The use of indigenous cattle in terminal cross-breeding to improve beef cattle production in Sub-Saharan Africa. Anim Genet Res 46:33–39

Sejian V, Samal L, Haque N, Bagath M, Hyder I, Maurya VP, Bhatta R, Ravindra JP, Prasad CS, Lal R (2015) Overview on adaptation, mitigation and amelioration strategies to improve livestock production under the changing climatic scenario. In: Sejian V, Gaughan J, Baumgard L, Prasad C (eds) Climate change impact on livestock: adaptation and mitigation. Springer, New Delhi

Sejian V, Bhatta R, Gaughan JB, Dunshea FR, Lacetera N (2018) Review: adaptation of animals to heat stress. Animal 12:S2:s431–s444

Seo SN, Mendelsohn R (2008a) Measuring impacts and adaptations to climate change: a structural Ricardian model of African livestock management. Agric Econ 38(2):151–65

Seo SN, Mendelsohn R (2008b) Animal husbandry in Africa: climate change impacts and adaptations. Afr J Agric Resour Econ 2(311-2016-5520):65–82

Seo SN, Mendelsohn R (2006) Climate change adaptation in Africa: a microeconomic analysis of livestock choice. CEEPA Discussion Paper No. 19, Centre for Environmental Economics and Policy in Africa, University of Pretoria, South Africa

Seré C, Van der Zijpp AJ, Persley G, Rege E (2007) Dynamics of livestock production systems, drivers of change and prospects for animal genetic resources. In: Proceedings of the first international technical conference on animal genetic resources for food and agriculture, 3–7 Sept 2007, Interlaken, Switzerland, pp 4–24

Shiawoya EL, Tsado DN (2011) Forage and fodder crop production in Nigeria: problems and prospects. World J Life Sci Med Res 1(4):88–93

Siddig K, Stepanyan D, Wiebelt M, Grethe H, Zhu T (2020) Climate change and agriculture in the Sudan: impact pathways beyond changes in mean rainfall and temperature. Ecol Econ 169:106566

Sikiru AB (2016) Assessment of feed resources utilization for livestock production by Agro Pastoralists in Tafa Local Government Area of Nigeria. J Rangel Sci 6(1):43–52. (1 Jan 2016)

Sikiru AB, Makinde OJ (2018) Effect of low-cost supplemental feeding practices on pre-weaning weight gain of goat kids in Tafa LGA Nigeria. Int J Agric Res Sustain Food Suffic (IJARSFS) 5(1):237–247. (16 Feb 2018)

Sikiru AB, Yousuf MB, Ademola SG (2018) Cassava Bran-Fish processing waste as dry season feed resources for sheep in Nigeria Southern Guinea Savannah. J Rangel Sci 8(1):11–22

Sikiru AB (2020) Livestock production at the nexus of resources competition and ethnoreligious cynicism in Nigeria-implicative analysis on food security. J Rangel Sci 10(3):267–281

Sikiru AB, Alemede IC, Arangasamy A, Egena SSA, Ijaiya AT (2020) Temperature elevation effects on livestock production-a study and forecast of Bengaluru climate data. Ecologia 10:1–8

Soto-Navarro SA, Krehbie CR, Duff GC, Galyean ML, Brown MS, Steiner RL (2000) Influence of feed intake fluctuation and frequency of feeding on nutrient digestion, digesta kinetics, and ruminal fermentation profiles in limit-fed steers. J Anim Sci 78:2215–2222

Srikanth K, Kumar H, Park W, Byun M, Lim D, Kemp S, tePas MFW, Kim J-M, Park J-E (2019) Cardiac and skeletal muscle transcriptome response to heat stress in Kenyan chicken ecotypes adapted to low and high altitudes reveal differences in thermal tolerance and stress response. Front Genet 10:993

Swanepoel PA, Tshuma F (2017) Soil quality effects on regeneration of annual Medicago pastures in the Swartland of South Africa. Afr J Range Forage Sci 34(4):201–208

Taye M, Lee W, Caetano-Anolles K, Dessie T, Hanotte O, Mwai OA, Kemp S, Cho S, Oh SJ, Lee H, Kim H (2017) Whole genome detection of signature of positive selection in African cattle reveals selection for thermotolerance. Anim Sci J 88:1889–1901

Thornton PK, van de Steeg J, Notenbaert A, Herrero M (2009) The impacts of climate change on livestock and livestock systems in developing countries: A review of what we know and what we need to know. Agric Syst 101(3):113–127

Thornton PK, Herrero M (2010a) Potential for reduced methane and carbon dioxide emissions from livestock and pasture management in the tropics. Proc Natl Acad Sci 107(46):19667–19672

Thornton PK, Herrero M (2010b) The inter-linkages between rapid growth in livestock production, climate change, and the impacts on water resources, land use, and deforestation. The World Bank

Traore S, Owiyo T (2013) Dirty droughts causing loss and damage in Northern Burkina Faso. Int J Global Warm 5(4):498–513

Vetter S, Goodall VL, Alcock R (2020) Effect of drought on communal livestock farmers in KwaZulu-Natal, South Africa. Afr J Range Forage Sci 37(1):93–106

Warimwe GM, Gesharisha J, Carr BV, Otieno S, Otingah K, Wright D, Charleston B, Okoth E, Elena L-G, Lorenzo G, Ayman E-B, Alharbi NK, Al-Dubaib MA, Brun A, Gilbert SC, Nene V, Hill AVS (2016) Chimpanzee adenovirus vaccine provides multispecies protection against Rift Valley fever. Sci Rep 6:20617. https://doi.org/10.1038/srep20617

Woldeamlak B, Radeny M, Mungai C (2015) Agricultural adaptation and institutional responses to climate change vulnerability in Ethiopia. CCAFS Working Paper no. 106. CGIAR Research Program on Climate Change, Agriculture and Food Security (CCAFS). Copenhagen, Denmark. www.ccafs.cgiar.org

Yaméogo ND, Nabassaga T, Ncube M (2014) Diversification and sophistication of livestock products: the case of African countries. Food Policy 49(2):398–407

Zougmoré R, Partey S, Ouédraogo M, Omitoyin B, Thomas T, Ayantunde A, Ericksen P, Said M, Jalloh A (2016) Toward climate-smart agriculture in West Africa: a review of climate change impacts, adaptation strategies and policy developments for the livestock, fishery and crop production sectors. Agric Food Secur 5(26). https://doi.org/10.1186/s40066-016-0075-3

Chapter 14
Mapping and Assessing the Seasonal Dynamics of Surface Urban Heat Intensity Using LandSAT-8 OLI/TIRS Images

Oluibukun Gbenga Ajayi [iD], **Tosin Sandra Kolade** [iD], **and Mahmud Baba** [iD]

Abstract Increased heat intensity in urban climate has serious implications on human health, contributing to urban liveability and vitality. As a way of mitigating the effect of excessive heat temperature in the urban area, it is imperative to examine the level of surface temperature in urban areas over time so that the urban heat intensity and its attendant consequences can be put into consideration when undertaking sustainable urban planning. This study examined the spatiotemporal dynamics of surface urban heat intensity in Bosso Local Government Area of Niger State using remotely sensed images. Landsat-8 OLI/TIRS images of the year 2015, 2017, 2019, and 2021 for both dry and wet seasons were used to determine the study area's Normalized Difference Vegetation Index (NDVI), surface emissivity, land surface temperature (LST), and Normalized Difference Built-up Index (NDBI), using ArcGIS 10.8 software. The result showed that a rise in built-up density, surface emissivity, and a decrease in vegetation density yields an increase in LST, while vegetation density proved to be of little effect in dry season when compared to the rainy season because most vegetation experiences draught at this time of the year. The result also showed that LST is higher in rainy season than it was in dry season because the wind, which decreases the effect of LST, is weak at this season of the year. The least value for surface emissivity in dry season was recorded to be 0.98605 while that of rainy is 0.98698, which implies that the emissivity of materials in the study area was observed to be higher in the rainy season than dry season. Furthermore, the result affirmed that a rise in urbanization gives rise to LST, likewise an increase in vegetation density of an area will lead to a decrease in the area's urban heat intensity.

O. G. Ajayi (✉)
Department of Land and Spatial Sciences, Namibia University of Science and Technology, Windhoek, Namibia
e-mail: oajayi@nust.na; gbenga.ajayi@futminna.edu.ng

O. G. Ajayi · T. S. Kolade · M. Baba
Department of Surveying and Geoinformatics, Federal University of Technology, Minna, Nigeria
e-mail: tosin.kolade4@gmail.com

M. Baba
e-mail: Mahmud.baba@futminna.edu.ng

The results also proved that wet periods can be hotter than dry periods of the year due to the presence of weak winds.

Keywords Normalized difference vegetation index · Land surface temperature · Surface emissivity · Normalized difference built-up index

Introduction

The atmospheric systems and energy balance of the earth are gradually being altered as a result of chaotic urbanization, which has a direct impact on human thermal discomfort. Such issues are exacerbated in the cities, since the urban environment is the object of man's most arbitrary landscape-modifying actions (Gomes and Caracristi 2021). In the light of the challenges of global warming and its characterizing dynamics related to earth's surface alterations, such as agricultural expansion, desertification, urban development, and so on, examining the surface urban heat intensity is critical. In this regard, a lot of effort has gone into determining land surface temperature using remote sensing data (Garouani et al. 2021). The removal of vegetation within urban areas, changes in urban thermal and physical properties of construction materials, building, morphology, surface roughness, urbanization and anthropogenic heat sources, all modifies, alters, or affects local energy and leads to increase in atmospheric temperature in urban areas compared to their surroundings (Ayanlade et al. 2021). Adequate and accurate information about the status of the land surface temperature (LST) of specific areas of interest is required for successful geo-environmental management, which involves the monitoring and modelling of the environment (Agbor and Makinde 2018). There are many natural and anthropogenic factors responsible for the increase or decrease in LST, while the degree of LST is seasonal and location dependent. Climate change and urbanization have been reported as one of the critically significant factors responsible for the change in land use and LST (Argueso et al. 2015; Elhadi et al. 2020).

The heat intensity effect of solar radiation varies significantly across urban and rural areas. It has been observed to be higher in urban or metropolitan areas than in rural areas. The term urban heat island (UHI) is used to describe this phenomenon, which is primarily impacted by the amount of plant and water pervious surfaces present in an urbanized area. Because water pervious surfaces and vegetation have been replaced by impervious surfaces in urban environments, there is less evaporation to reduce LST (Michael et al. 2012).

In an urban environment, natural vegetation is eliminated and replaced by non-transpiring and non-evaporating surfaces that have low capacity for solar reflectivity and high capacity for heat absorption such as concrete, asphalt, and metals in most cases, resulting in a significant modification of the earth's surface (Andrew 2012; Ridwan et al. 2021). This change eventually causes incoming solar energy to be redistributed, resulting in the rural–urban disparity in air temperatures and surface radiance (Guiling et al. 2008).

The influence of urbanization is tremendous, and it affects or alters the natural ecosystem; therefore, understanding UHI is vital for a variety of applications in earth

and physical sciences as well as environmental management techniques (Aneeqa et al. 2016). The demand for agricultural production, food, and shelter is increasing as the global population grows. As a result of anthropogenic activities, land cover characteristics are shifting to satisfy rising population need and replacing vegetated areas with impermeable surfaces, inadvertently leading to climate change (Imran et al. 2021). Increased heat intensity in the urban climate has major consequences on human health and the usage of outdoor areas, as well as many activities that contribute to the liveability and vitality of cities. It causes different multifaceted issues such as skin cancer and greater energy consumption because air conditioners are often required (Michael et al. 2012; Naserikia et al. 2019).

LST is defined by how hot the "surface" of the earth would feel when touched in a particular region (Przyborski 2021) while the surface in this context and as used in satellite remote sensing refers to whatever a satellite observes as its signal pierces through the atmosphere to the earth. Surface heat fluxes, which are affected by urbanization, influence the LST in an area (Dousset and Gourmelon 2003). Therefore, understanding the spatiotemporal distribution of LST will aid in deciphering its mechanism and determining possible mitigation techniques (Sun et al. 2009).

Apart from the LST, other indices that have been reported to contribute to the urban heat island of a location include vegetation which is often measured using the Normalized Difference Vegetative Indices (NDVI), urbanization or built-up areas which is often measured using the Normalized Difference Building Indices (NDBI), surface emissivity, etc.

The NDVI is an index used to detect and ascertain the existence or presence of live green vegetation. Most visible light (0.4–0.7 m) is absorbed by healthy vegetation, whereas most near-infrared light (0.7–1.1 m) is reflected. In contrast, unhealthy or sparse vegetation will reflect less near-infrared light and more visible light (Weirer and Herring 2010). As a result, greater radiation that is reflected in the near-infrared wavelengths than the visible wavelengths indicates the existence of green vegetation, while minimal variation in intensity between the two wavelengths suggests the existence of either non-vegetated surfaces or sparse vegetation (Weirer and Herring 2010). The built-up density for each area is described by the NDBI, which is synonymous to the vegetation density described by the NDVI. The ratio of short red infrared (SWIR) to near infrared (NIR) is calculated as NDBI, with indices ranging from −1 to 1 (Kshetri 2018).

The impact of the relationship or connection between the NDVI and LST, especially in locations where the urban heat intensity phenomenon is more prevalent and mitigating efforts are required, cannot be overemphasized. This is primarily because denser vegetation lowers LST by ensuring the transfer of latent heat to the atmosphere from the surface via evapotranspiration. The NDVI is used to investigate this relationship and, as a result, provides insight into how plants or vegetation's natural cooling mechanism can be exploited to improve urban thermal settings. In general, it is expected that lower LSTs are recorded or observed in locations or places with a high NDVI, implying that the two have an indirect relationship. However, surface evapotranspiration and soil moisture levels may significantly alter or modify the dynamics of this relationship (Yuan and Bauer 2007).

A property or attribute of a surface that determines the volume of energy that is emitted by an object at a particular temperature when compared to a blackbody at the same temperature is known as surface emissivity (EXERGEN 2021). It can also be described as the ability of a surface or an object to convert heat energy it receives into radiant energy (Sekertekin and Bonafoni 2020). The emissivity is gotten from NDVI after the fractional vegetation (Pv) cover has been estimated and then calculated from the reflectance values of the materials on the earth surface based on the results of the NDVI. The emissivity of materials on the earth's surface reflects how well they absorb all incident radiation and convert it to internal energy before emitting (re-radiating) the received energy at the highest rate feasible per unit area (Isa et al. 2016).

One of the important features or characteristics that can be observed by satellite remote sensing is the surface temperature of an area. This data (surface temperature) has a wide range of applications in ecology, environmental studies as well as spatial data modelling, which is frequently employed in web-based GIS applications (Sameen and Al Kubaisy 2014).

Recently, the connection and correlation between LST and other factors or indices have received significant research attention (Peng et al. 2020). Researchers frequently look into the individual interaction between LST, vegetation, surface emissivity, and water, as well as the impact of urban land growth on temperature change, while little known effort has been invested in the combined effects of some of these interactions, a gap this research seeks to fill. The fundamental goal of this study is to investigate the combined effect and interdependence of vegetation (using the Normalized Difference Vegetation Index (NDVI)), built-up area (using Normalized Difference Built-up Index (NDBI)), surface emissivity, and the LST in the assessment of urban heat intensity using Bosso Local Government Area of Niger State, Nigeria, as a case study.

Materials and Methods

Bosso, which is the project site of this study, is one of the Local Government Areas (LGA) in Niger State, Nigeria (see Fig. 14.1). With its administrative headquarters situated in Maikunkele, it covers an area of about 1592 km^2 and a population of about 147,359 according to the 2006 census. Bosso LGA has a high heat flow (Mohammed et al. 2019) which could be as a result of increased urban activities, hence, making it a suitable location for this study.

The study area experiences both wet (rainy) and dry seasons annually, and an attempt was made to assess the effect of seasonal variation of the LST or the heat intensity of the study area. Therefore, two images were downloaded for each year: one at dry season (February) and the second at rainy season (September), for the years 2015, 2017, 2019, and 2021, making a total of eight images. The properties of the Landsat-8 images, generated from their metadata, are presented in Table 14.1.
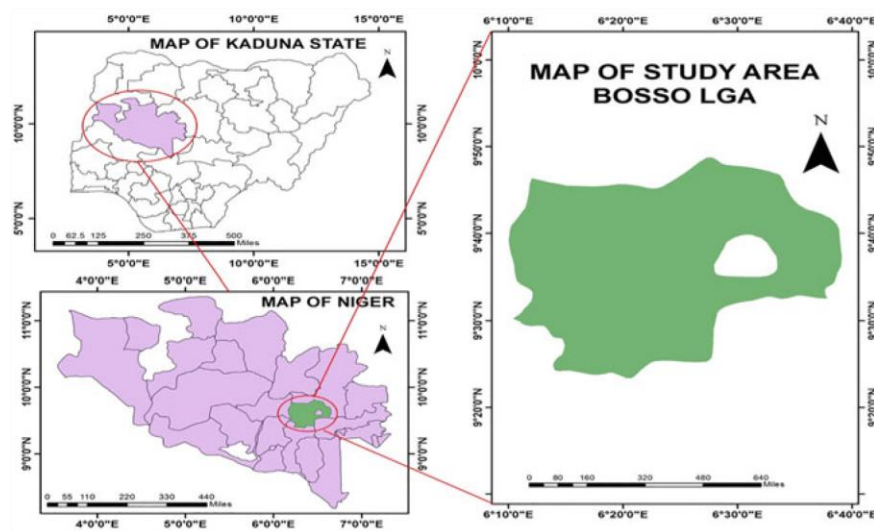
Fig. 14.1 Cartographic description of the study area

Table 14.1 Characteristics of the used Landsat-8 OLI images

Data	Sensor	Bands	Resolution/grid cell size	Season	Date obtained	Year
Landsat-8	OLI	11	30 m	Dry	25-02-2015	2015
Landsat-8	OLI	11	30 m	Rainy	21-09-2015	2015
Landsat-8	OLI	11	30 m	Dry	14-02-2017	2017
Landsat-8	OLI	11	30 m	Rainy	26-09-2017	2017
Landsat-8	OLI	11	30 m	Dry	20-02-2019	2019
Landsat-8	OLI	11	30 m	Rainy	27-05-2019	2019
Landsat-8	OLI	11	30 m	Dry	25-02-2021	2021
Landsat-8	OLI	11	30 m	Rainy	21-09-2021	2021

OLI = Operational land imager

The step-by-step or detailed procedure adopted for the execution of this study is presented in Fig. 14.2. The used Landsat-8 OLI/TIRS C2 L1 band images for 2015, 2017, 2019, and 2021 were downloaded from https://earthexplorer.usgs.gov/.

Radiometric and Atmospheric Correction

On satellite images, radiometric and atmospheric correction is frequently used to reduce the atmosphere's absorption and scattering effects. As the electromagnetic (EM) energy travels from the sun to the earth and back to the sensor, through the
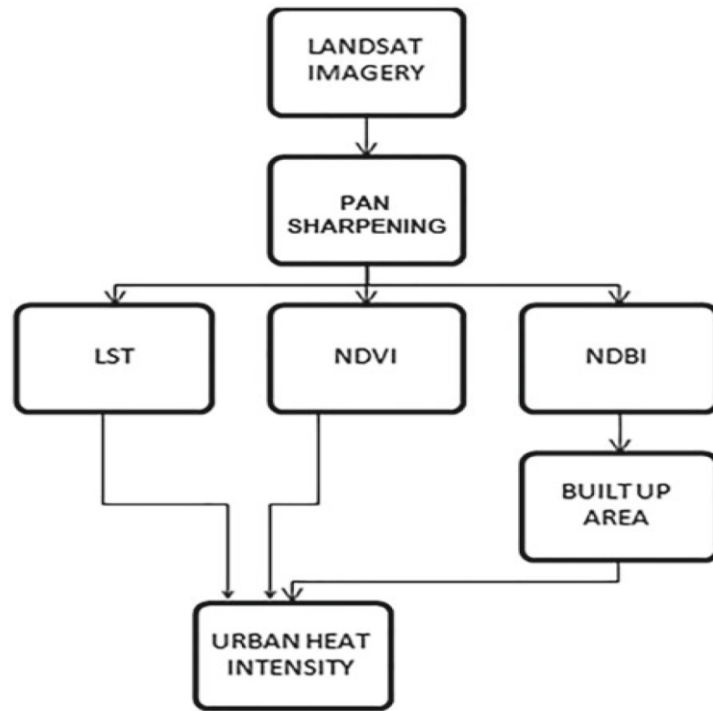
atmosphere, absorption diminishes the intensity of EM energy resulting in haziness, while the energy is redirected in the atmosphere by scattering resulting in an adjacent effect in which neighbouring pixels are shared and thus affecting image quality (GISgeography 2021). Radiometric and atmospheric correction removes the effect of sensor influence and atmospheric effect on the reflectance value of satellite images. Radiometric and atmospheric correction was done by computing the Top of Atmospheric (TOA) spectral reflectance (Eq. 14.1), followed by the correction of sun angle (Eq. 14.2) for all the satellite images downloaded for this study.

Procedure for Obtaining LST

LST can be estimated using the Landsat-8 OLI/TIRS C2 L1 thermal bands by applying Eqs. (14.1)–(14.8) (Rosado et al. 2020) presented in the simplified procedure described by the following five (5) steps.

I. Top of Atmospheric (TOA) spectral reflectance.

On a given surface, the ratio of reflected solar radiation to incident solar radiation is often referred to as the ratio of TOA radiance (Eq. 14.1), which is a unitless measurement. The mean solar spectral irradiance and the solar zenith angle derived

from satellite-measured spectral radiance are used for the estimation of TOA (Rosado et al. 2020).

$$TOA(L) = ML * Qcal + AL \tag{14.1}$$

where M_L is the band-specific multiplicative rescaling factor from the metadata, Q_{cal} corresponds to band 10, and A_L is the band-specific additive rescaling factor from the metadata.

II. Calculation of Brightness Temperature

The thermal band detectors record TOA's brightness temperature in the form of digital numbers (DNs), which is then converted to surface temperature using the single channel algorithm. Surface temperatures obtained with Eq. (14.3) are deemed to be highly accurate (Michael et al. 2012).

$$BT = (K2/(ln(K1/L) + 1)) - 273.15 \tag{14.2}$$

where K_1 and K_2 are the band-specific thermal conversion constant from the metadata and L is the TOA. In order to obtain the results in degree Celsius, absolute zero is added to the radiant temperature as presented in Eq. (14.3).

$$BT = \big(1321.0789/Ln\big((777.8853/''\%TOA\%'') + 1\big)\big) - 273.15 \tag{14.3}$$

III. Extracting the NDVI

Reflectance data of Landsat-8 images, i.e. the visible red (Red) and the near-infrared (NIR) bands (bands 4 and 5, respectively) were used to extract the NDVI.
    The NDVI was extracted using the expression presented in Eqs. (14.4) and (14.5).

$$NDVI = (Band\ 5 - Band\ 4)/(Band\ 5 + Band\ 4) \tag{14.4}$$

It should be noted that calculating the NDVI is crucial since it is necessary to estimate the proportion of vegetation (Pv), which is related to the NDVI, and emissivity (ε), which is related to the proportion of vegetation.

$$NDVI = Float(Band\ 5 - Band\ 4)/Float(Band\ 5 + Band\ 4) \tag{14.5}$$

IV. Estimating vegetation proportion (P*v*)

The proportion of vegetation was estimated using Eq. (14.6) (Carlson and Ripley 1997).

$$Pv = Square((NDVI - NDVImin)/(NDVImax - NDVImin)) \tag{14.6}$$

The minimum and maximum values of the NDVI are gotten from the properties of NDVI under the source tab or the highest and lowest value range in ArcGIS 10.8.

V.   Estimating Surface Emissivity (ε)

The effectiveness of a material's surface in emitting energy as thermal radiation is known as its emissivity. Thermal radiation is electromagnetic radiation that includes both visible (light) and infrared (infrared) wavelengths that are invisible to the human eye (Sobrino et al. 2013). The mathematical expression used for the estimation of emissivity is presented in Eq. (14.7).

$$\varepsilon = m * Pv + n \qquad (14.7)$$

where m = emissivity of vegetation (0.004), Pv = percentage of vegetation, and n = soil emissivity value (0.986).

VI   Estimating the Land Surface Temperature

Equation (14.8) presents the mathematical expression used for the estimation of LST.

$$LST = (BT/(1 + (0.00115 * BT/1.4388) * Ln(\varepsilon))) \qquad (14.8)$$

where BT = Brightness temperature and ε = Emissivity.

Estimating the NDBI

The NDBI was extracted using the reflectance data (short red infrared (SWIR) and near infrared (NIR) bands) of Landsat-8 images. The NDBI is estimated as the ratio between short red infrared (SWIR) and near infrared (NIR) and has indices ranging from −1 to 1. Generally, the mathematical expression for estimating the NDBI for an area is shown in Eq. (14.9), while Eq. (14.10) presents the equation used to extract the NDBI specifically from Landsat-8 image.

$$NDBI = (SWIR - NIR)/(SWIR + NIR) \qquad (14.9)$$

$$NDBI = float(band\ 6 - band\ 5)/float(band\ 6 + band\ 5) \qquad (14.10)$$

where band 6 is a SWIR band and band 5 is a NIR band. Built-up areas were extracted from the built-up density in the form of point features for clear depiction of urbanization.

Interpretation of NDBI and NDVI

Generally, the value of the NDBI and NDVI calculation ranges from −1 to 1. The representation of the values within the range for NDVI is presented in Table 14.2,

Table 14.2 NDVI value range and feature represented (Kshteri 2018)

NDVI value range	Feature represented
−1–0	Water bodies
−0.1–0.1	Snow, barren rocks, or sand
0.2–0.5	Senescing crops, grasslands, or shrubs
0.6–1.0	Tropical rainforest or dense vegetation

Table 14.3 NDVI value range and the represented state of plant's health

| NDVI value range	State of plant
−1–0	Inanimate objects or plants that are dead
0–0.33	Plants that are unhealthy
0.33–0.66	Plants that are moderately healthy
0.66–1	Plants that are very healthy

while Table 14.3 presents the range of index values representing the state of plant health (EOS 2019). For the NDBI, while negative values represent non-urban land areas, urban land areas are represented by positive values.

Results and Discussion

For clearer presentation, the results were presented and discussed in two subsections. While the results obtained in the seasonal dynamics of the surface heat intensity of the study area in the dry season were presented in subsection "Surface Heat Intensity of the Area in the Dry Season", the result obtained for the same analysis in the rainy season was presented in subsection "Surface Heat Intensity of the Area in the Rainy Season". The relationships and effects of the combined indices (NDVI, NDBI, and LST) on the surface urban heat intensity are also presented.

Surface Heat Intensity of the Area in the Dry Season

Maps depicting the spatial distribution of NDVI, NDBI, and the spatial variation of LST values of the study area for the dry season are presented in Figs. 14.3, 14.4 and 14.5, respectively, while Table 14.4 contains the estimated maximum values of the NDBI, NDVI, and LST obtained for 2015, 2017, 2019, and 2021 for the dry season. From the results, it was observed that in dry season, the highest maximum value of LST was recorded in the year 2017 (51 °C) which also yielded the highest NDVI and NDBI values of 0.388 and 0.577, respectively, while the lowest maximum value of LST was recorded in the year 2015 (33 °C).
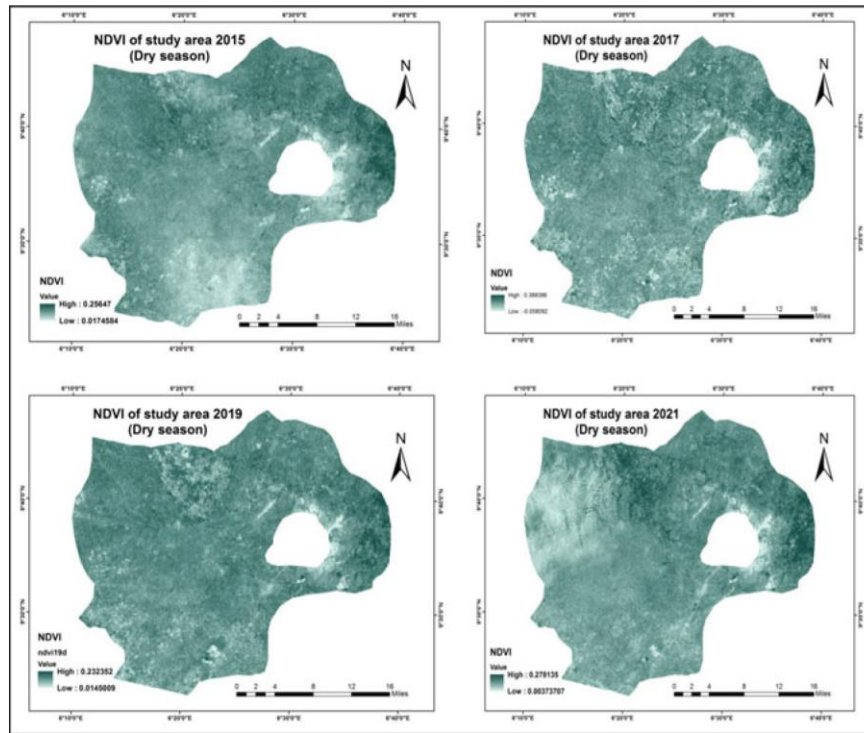
Fig. 14.3 Spatial distribution of NDVI in dry season

Also, the value for LST is lowest in the year 2015, but its value for NDBI (0.425) is higher than the values recorded for the years 2019 and 2021 which are 0.414 and 0.320, respectively, while the vegetative index value for the year 2021 (0.278) is higher than that of the year 2015 (0.257). Therefore, the lowest LST in the dry season over the years understudied is justifiably expected to be reported in the year 2021 since vegetation reduces the effect of LST, and the value of the NDBI recorded for the year 2021 is the least compared to other years. Also, since NDVI value below 0.5 indicates the presence of shrubs, rocks, sand, unhealthy plants, grasses (unhealthy or moderately healthy), etc., and the highest maximum value for NDVI in dry season is 0.388 as recorded in the year 2017, it evidently shows that most plants within the study area have already dried up at this time of the year; therefore, the effect of NDVI in dry season is minimal.

Also, since surface emissivity contributes to surface temperature in an area along with built-up index, the surface emissivity of the study area was examined for each of the years understudied for the dry season, and the obtained result is presented in Fig. 14.6. The maximum surface emissivity recorded in the years 2017 and 2021 illustrates the extent to which various materials, such as bare land or soils, engineering structures, metal, concrete, and tar, absorb all incident radiation completely, and convert it to internal energy. The absorbed energy is then emitted (re-radiated) into
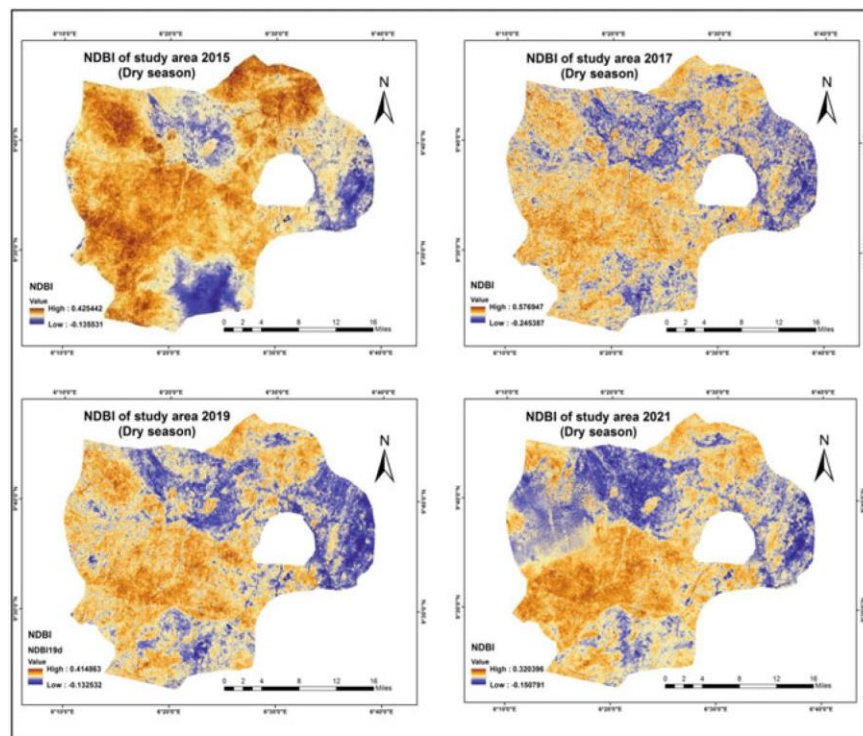
Fig. 14.4 Spatial distribution of NDBI in dry season

the atmosphere and thereby contributing to LST. The recorded surface emissivity in the years 2017 and 2021 is higher than that of the year 2015 for the dry season which explains why the least value of LST for dry season was recorded in the year 2015 and not in 2021. It also explains why LST in the year 2021 is higher than what it was in the year 2019.

Surface Heat Intensity of the Area in the Rainy Season

Figures 14.7, 14.8 and 14.9 present the graphical description of the spatial distribution of NDVI, NDBI, and the spatial variation of LST of the study area for the rainy season, respectively. The estimated maximum values of the NDBI, NDVI, and LST obtained for the years 2015, 2017, 2019, and 2021 for the rainy season are presented in Table 14.5. Similar to what was observed in the results obtained for the dry season, the lowest value of LST was recorded in the year 2021, but its value for built-up index (0.267) is higher than NDBI values for the years 2017 and 2015 which are 0.259 and 0.243, respectively. Also, the year 2019 had the highest maximum value for LST (70 °C), while the year also recorded the lowest NDVI value of 0.544 and the highest
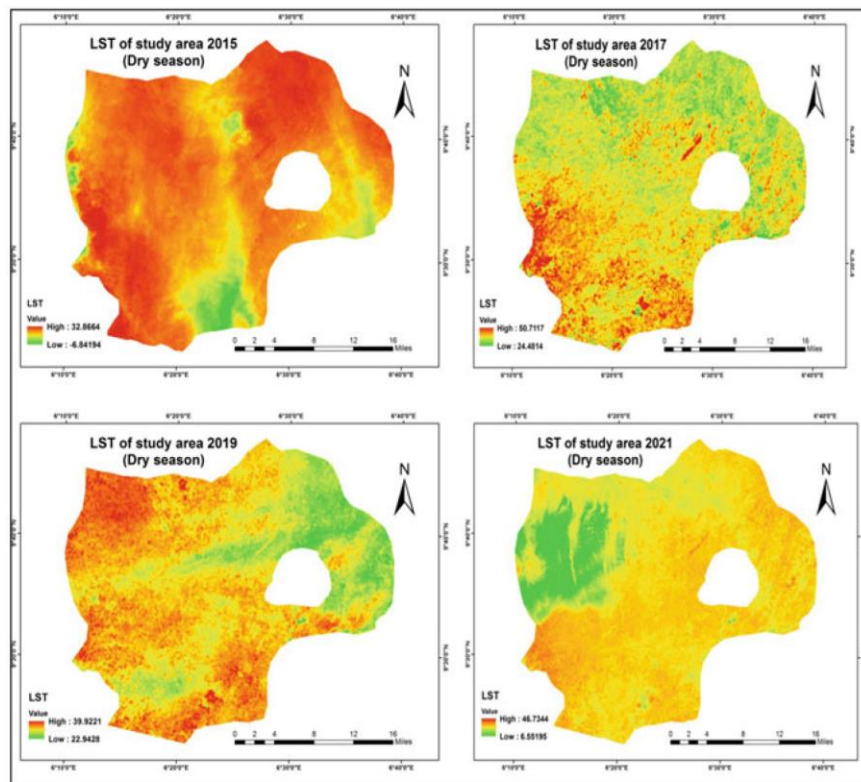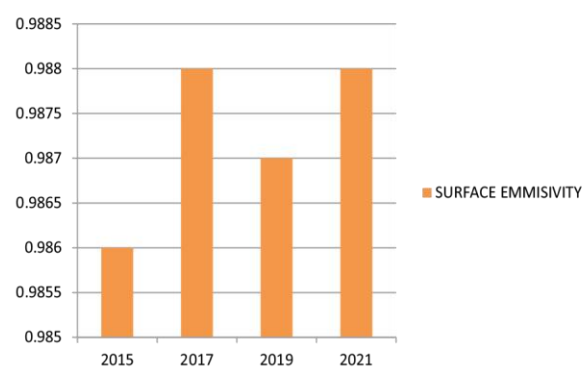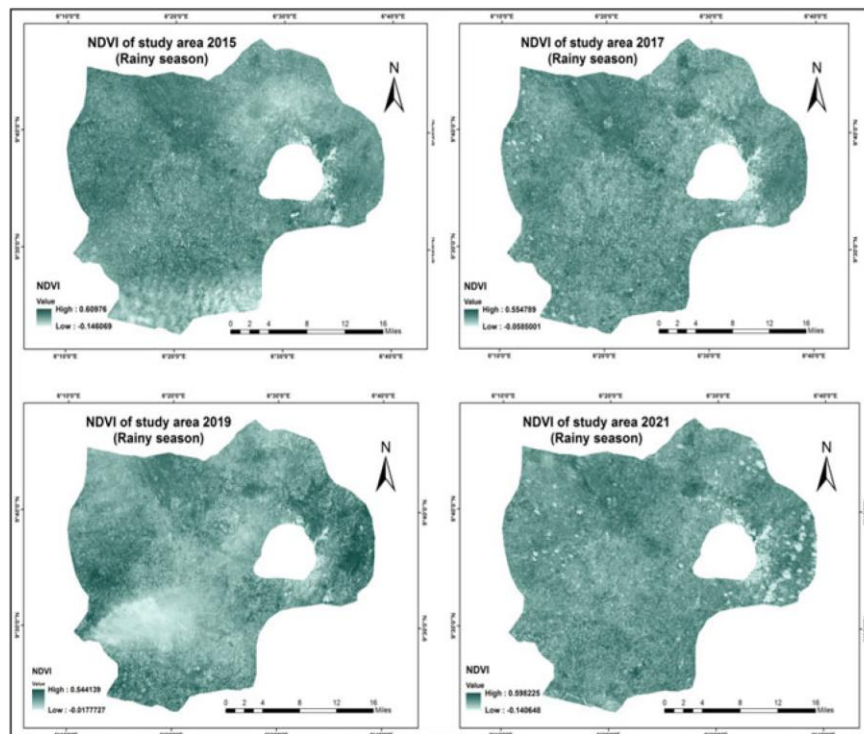
Fig. 14.5 Spatial variation of LST in dry season

Table 14.4 Estimated NDVI, NDBI, and LST maximum values for the dry seasons

Year	NDVI	NDBI	LST (°C)
2015	0.257	0.425	33
2017	0.388	0.577	51
2019	0.232	0.414	40
2021	0.278	0.320	47

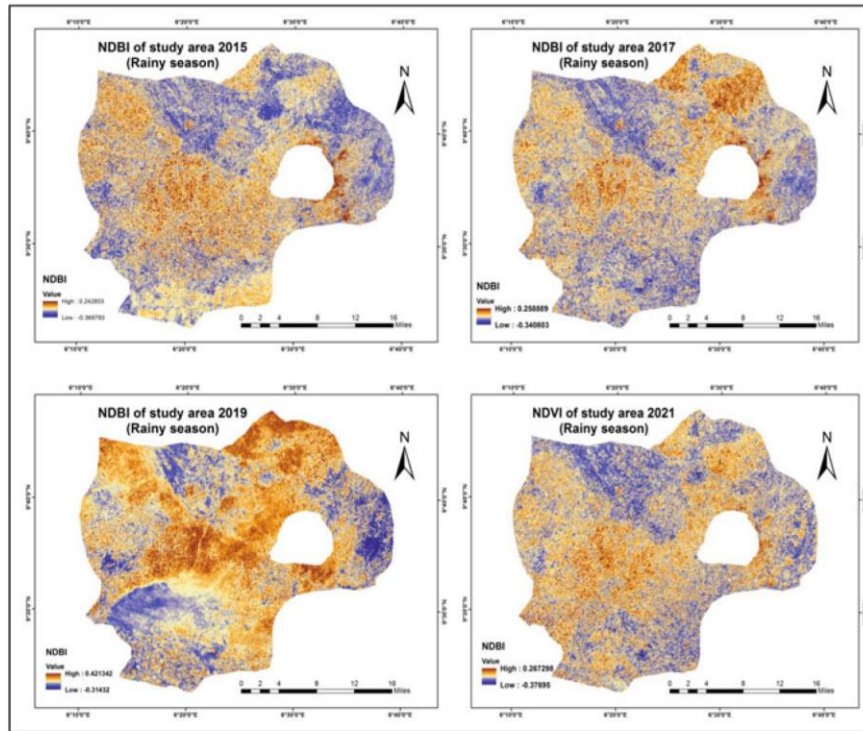**Fig. 14.6** Surface emissivity in dry season

Fig. 14.7 Spatial distribution of NDVI in rainy season

NDBI value of 0.421. The implication of this is that in the year 2019, urbanization rate was very high which had a negative effect on vegetation thereby increasing the urban heat intensity of the study area in the rainy season. In contrast, for the year 2021, there was a very low heat intensity judging by the recorded lowest maximum value for LST of 29 °C. This can be attributed to the high NDVI of 0.598 and low NDBI of 0.267, which implies an improvement in vegetation growth and reduced urban growth, respectively.

Although the vegetation index for the years 2021 and 2015 is very close, the lowest value of LST recorded in the rainy season of the year 2015 is justified by the lowest value for built-up index recorded in the same season and the highest value of the NDVI recorded in the dry season over the studied time epochs. This suggests that while there are low or reduced urbanization activities, there were high vegetated activities which led to the recorded low LST within the period of study.

Also, the surface emissivity of the study area in the rainy season was examined over the studied years and the result is presented in Fig. 14.10. Similar to the surface emissivity of the study area in the dry season, the surface emissivity for the years 2015 and 2017 was observed to be considerably higher than what it was in the years 2019 and 2021 in the rainy season, which explains why the least value of LST for the rainy season was recorded in the year 2021 and not in year 2015.

Fig. 14.8 Spatial distribution of NDBI in rainy season

Generally, it was observed from the analysis that the surface emissivity values of the study area obtained in the rainy season were significantly higher than the surface emissivity values of the study area obtained for dry season across all the years, except for the results obtained for the year 2019. This is because the strength of wind in the study area is weak at this season of the year.

Conclusion

This research shows the potential of using Geographic Information System (GIS) and remote sensing techniques in assessing the surface heat intensity of any location. The findings of this study affirmed that a rise in surface urban heat intensity is resulted from an increase in urbanization and a decrease in vegetation. The effect of increased built-up density and surface emissivity which resulted to an increase in LST proves that increase in urbanization leads to an increase in surface heat intensity. The study also proved that a rise in vegetation density leads to a decrease in urban heat intensity and that the effect is more significant in the rainy season than dry season as vegetation is usually dry at this season of the year, where soil moisture content is low. In as

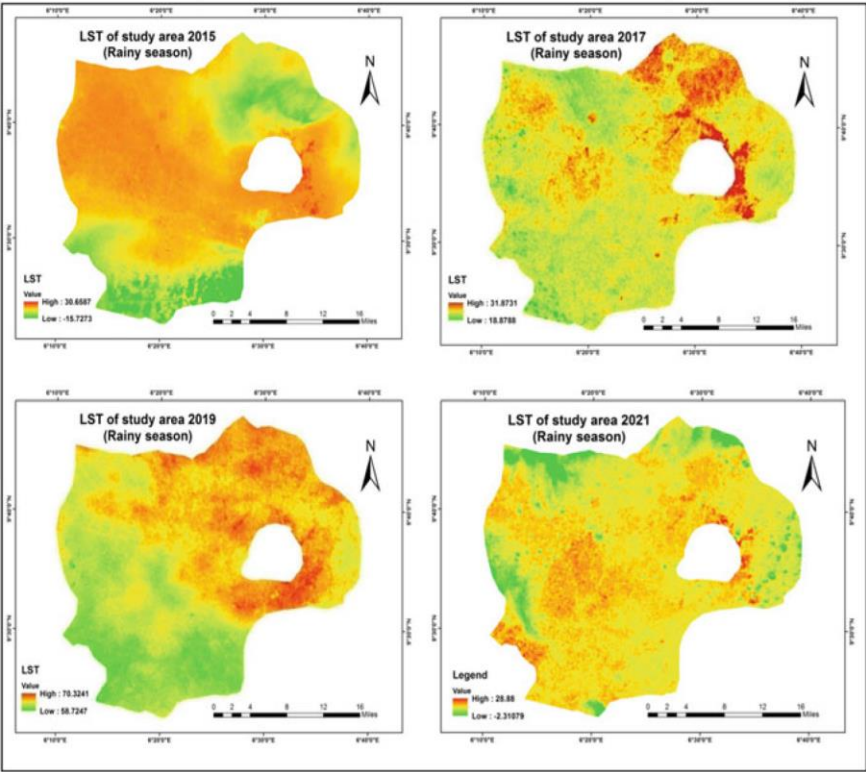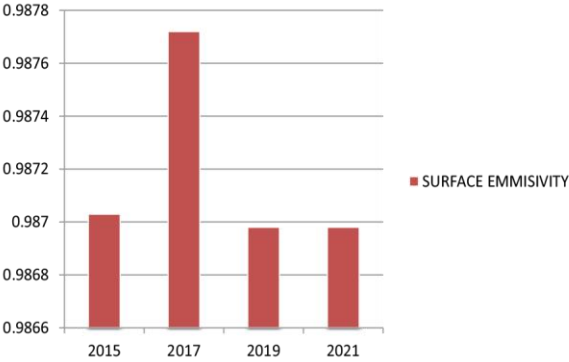**Fig. 14.9** Spatial variation of LST in rainy season

Table 14.5 Estimated NDVI, NDBI, and LST maximum values for the rainy seasons

Year	NDVI	NDBI	LST (°C)
2015	0.610	0.243	31
2017	0.555	0.259	32
2019	0.544	0.421	70
2021	0.598	0.267	29

Fig. 14.10 Surface emissivity in rainy season

much as vegetation is more effective in rainy season, wet periods are usually periods of high urban heat intensity because of the high emissivity values associated with this season. This is because wind, which decreases the effect of urban heat intensity, is weak at this season of the year. Further studies will attempt to investigate the effect of other factors such as terrain elevation or topography and presence of water bodies on the urban heat intensity of the study area.

References

Agbor CF, Makinde EO (2018) Land surface temperature mapping using Geoinformatics techniques. Geoinform FCE CTU 17(1):2–17. https://doi.org/10.14311/gi.17.1.2

Andrew F (2012) Exploring the relationship between land surface temperature and vegetation abundance for urban heat island mitigation in Seville, Spain. LUMA-GIS Thesis Nr 15:1–58

Aneeqa A, Muhammad AB, Khadija N, Huma A (2016) Assessment of Urban Heat Island (UHI) using remote sensing and GIS. Glob J Hum-Soc Sci 2(2):1–9

Argueso D, Evans JP, Pitman AJ, Luca A (2015) Effects of city expansion on heat stress under climate change conditions. PLoS One 10(2), Article ID:e0117066

Ayanlade A, Aigbiremolen M, Oladosu O (2021) Variations in urban land surface temperature intensity over four cities in different ecological zones. Sci Rep. https://doi.org/10.1038/s41598-021-99693-z

Carlson TN, Ripley DA (1997) On the relation between NDVI, fractional vegetation cover, and leaf area index. Remote Sens Environ 62:241–252

Dousset B, Gourmelon F (2003) Satellite multi-sensor data analysis of urban surface temperatures and landcover. ISPRS J Photogramm 58:43–54

EXERGEN Global industrial sales. (2021) What is emissivity? https://www.exergenglobal.com/tech-notes/31-what-is-emissivity

Elhadi KM, Yungang C, Guoxiang L, Moshbeh RK, Ashraf AB, Fawzi Z, Mohammed S (2020) Study for predicting land surface temperature (LST) using Landsat data: a comparison of four algorithms. Adv Civil Eng. https://doi.org/10.1155/2020/7363546

Garouani M, Amyay M, Lahrach A, Oulidi HA (2021) Land surface temperature in response to land use/cover change based on remote sensing data and GIS techniques: application to Saïss Plain, Morocco. J Ecol Eng 22(7):100–112

GIS Geography (2021) What is atmospheric correction in remote sensing? https://gisgeography.com/atmospheric-correction/

Gomes BY, Caracristi I (2021) Seasonal analysis on land surface temperature (LST) and normalized difference vegetation index (NDVI) variations in the Iguatu semi-arid hinterland, Ceará. Int J Hydrol 5(6):289–294

Guiling W, Weimei J, Ming W (2008) An assessment of urban heat island effect using remote sensing data. http://hdl.handle.net/1834/5876

Imran HM, Hossain A, Islam AKMS, Rahman A, Bhuiyan AE, Paul S, Alam A (2021) Impact of land cover changes on land surface temperature and human thermal comfort in Dhaka City of Bangladesh. https://doi.org/10.1007/s41748-021-00243-4

Isa Z, Baba I, Ayuba Z (2016) Estimation of Land Surface Temperature of Kaduna Metropolis, Nigeria using Landsat images. Sci World J 11(3):1–7

Kshetri T (2018) NDVI, NDBI & NDWI Calculation using LandSAT 7 and 8. https://www.linkedin.com/pulse/ndvi-ndbi-ndwi-calculation-using-landsat-7-8-tek-bahadur-kshteri

Michael SA, Saviour M, NaaDedei T (2012) Mapping land surface temperature and land cover to detect urban heat island effect: a case study of Tarkwa, South West Ghana. Department of Geomatics Engineering, University of Mines and Technology, P.O. Box 237, Tarkwa, Ghana

Mohammed A, Adewumi T, Kazeem AS, Abdulwaheed R, Adetona AA, Usman A (2019) Assessment of geothermal potentials in some parts of upper Benue trough Northeast Nigeria using Aeromagnetic data. J Geosci Eng Environ Technol 4(1). https://journal.uir.ac.id/index.php/JGEET/article/view/2090

Naserikia M, Shamsabadi EA, Filho WL (2019) The Urban Heat Island in an urban context: a case study of Mashhad, Iran. https://www.ncbi.nlm.nih.gov/pmc/articles/PMC6388183

Peng X, Wu W, Zheng Y, Sun J, Hu T, Wang P (2020) Correlation analysis of land surface temperature and topographic elements in Hangzhou, China. Scientific Rep. https://www.nature.com/articles/s41598-020-67423-6

Przyborski P (2021) Land surface temperature. Earth observatory. https://earthobservatory.nasa.gov/global-maps/MOD_LSTD_M

Ridwan, Rasyidi ES, Syafri, Rahman R, Okviyani N, Jumadil, Ma'rief AA (2021) Assessment of the relationship between building density and urban heat island using Landsat images in Makassar city. In: International conference on research collaboration of environmental science. https://doi.org/10.1088/1755-1315/802/1/012042

Rosado MRG, Guzman MEA, Lopez CJE, Molina MW, Garcia HLC, Yedra EL (2020) Mapping the LST (Land Surface Temperature) with satellite information and software ArcGis. In: International conference on research collaboration of environmental science. https://doi.org/10.1088/1757-899X/811/1/012045

Sameen IM, Al Kubaisy AM (2014) Automatic surface temperature mapping in ArcGIS using LANDSAT-8 TIRS and ENVI tools case study: Al Habbaniyah Lake. J Environ Earth Sci 12(4):1–7

Sekertekin A, Bonafoni S (2020) Land surface temperature. Retrieval from Landsat 5, 7, and 8 over Rural Areas: Assessment of Different Retrieval Algorithms and Emissivity Models and Toolbox Implementation. Retrieved from https://www.mdpi.com/2072-4292/12/2/294/htm

Sobrino J, Wang N, Wu H, Li ZL (2013) Land surface emissivity retrieval from satellite data. Int J Remote Sens 34(9–10):3084–3127. https://doi.org/10.1080/01431161.2012.716540

Sun Q, Tan J, Xu Y (2009) An ERDAS image processing method for retrieving LST and describing urban heat evolution: a case study in the Pearl River Delta Region in South China. Environ Earth Sci 1047–1055

Weirer J, Herring D (2010) Measuring vegetation (NDVI & EVI) (NASA Earth Observatory). http://earthobservatory.nasa.gov/Features/MeasuringVegetation/measuring_vegetation_2.php

Yuan F, Bauer ME (2007) Comparison of impervious surface area and normalized difference vegetation index as indicators of surface urban heat island effects in Landsat imagery. Remote Sens Environ 106:375–386